Nortek Technical Note No.: TN-021
Title: Chesapeake Bay AWAC Evaluation
Last Edited: October 5, 2004
Authors: Eric Siegel-NortekUSA, Chris Malzone-NortekUSA, Torstein Pedersen-Nortek AS
Number of Pages: 12

Chesapeake Bay AWAC Evaluation

Overview

The Nortek AWAC (integrated Acoustic Waves And Currents sensor) was deployed in 20 meters of water at the mouth of the Chesapeake Bay, just east of the Bay Bridge Tunnel. The AWAC was deployed roughly 100 m North of a Triaxys wave buoy located at 36° 57.531' N, 76° 00.924' W (Fig. 1 & 2).

The AWAC evaluation deployment lasted 12 days, beginning August 21st 2004 and ending September 1st 2004. The AWAC was set up to profile current velocities in 0.5 m cells every 6 minutes (with a 3 minute averaging window). Waves were measured in bursts of 2048 samples (at 2 Hz for 17 minutes) every 30 minutes, resulting in 546 wave files. Acoustic surface tracking (AST) was measured at 4 Hz. Zero checksum errors were logged.

The Triaxys wave buoy was configured to measure wave height and direction for the first 20 minutes of every hour. Below are the results comparing the Triaxys wave buoy with the AWAC.

Results

The weather during the 12 day deployment provided a variety of conditions in which to evaluate and compare the performance of the AWAC versus that of the Triaxys wave buoy. Figure 3 gives significant wave height (Hs) and maximum wave height (Hmax) for the AWAC and the buoy. Significant wave height was typically 0.5 to 1.0 m, with a broad peak at the end of August when Hurricane Gaston passed near the Chesapeake Bay. Significant wave heights during this period were nearly 1.5 m, with maximum wave heights reaching 2.5 m. Waves of this amplitude are infrequent in the Chesapeake Bay during the summer and are powerful enough to pose a hazard to most recreational boaters. Waves of this height could also affect the maneuvering, docking and loading of larger commercial and military vessels.

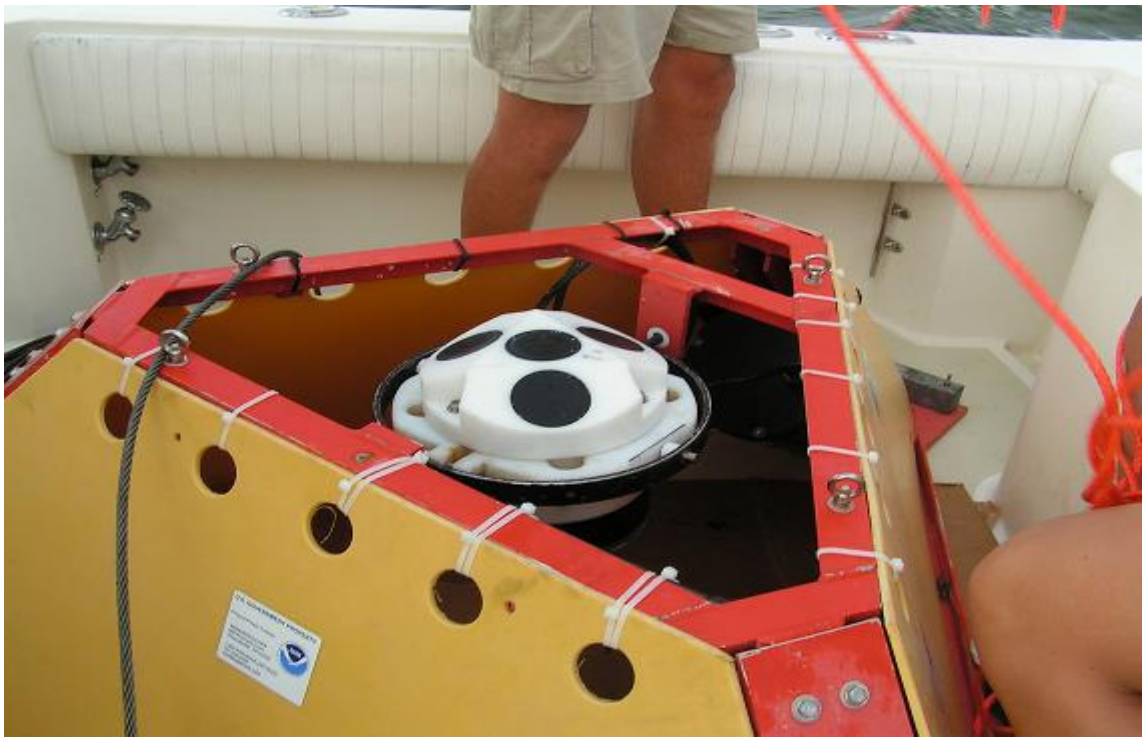

Figure 1. The AWAC was placed in a simple aluminum bottom mount frame with trawl-resistant sides affixed to the mount.

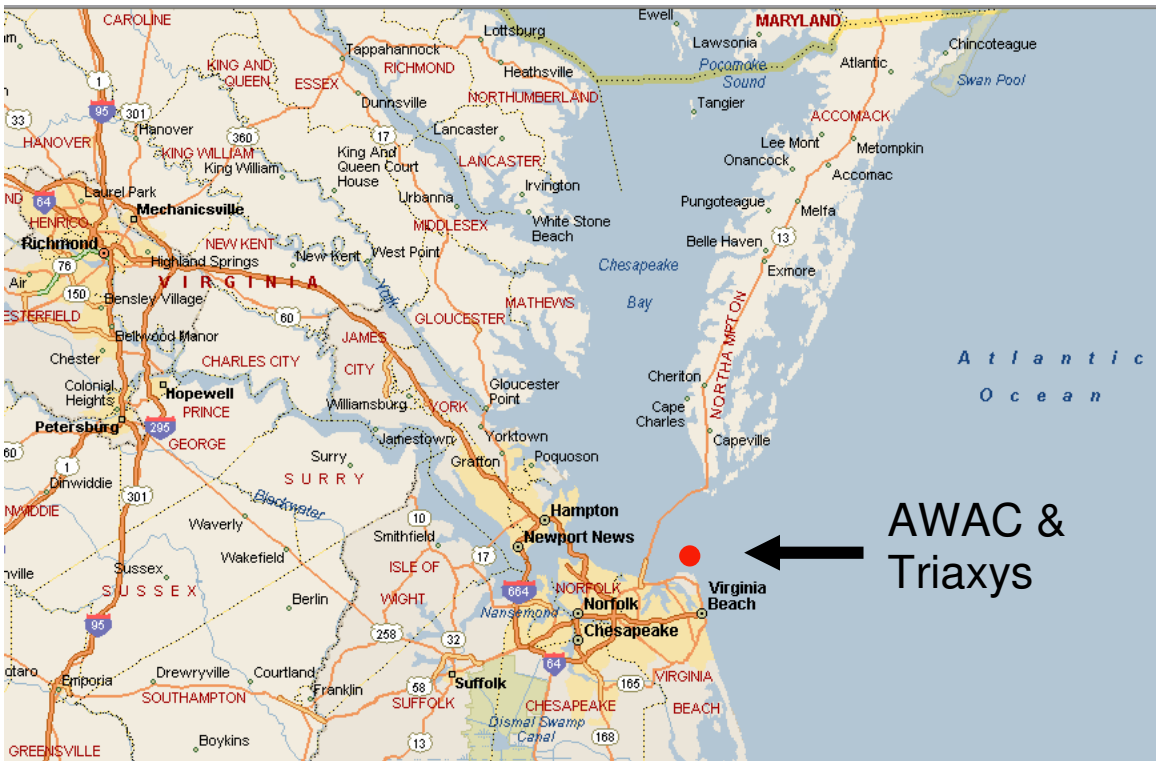

Figure 2. The AWAC and Triaxys wave buoy were deployed in 20 m of water near the mouth of the Chesapeake Bay, just east of the Bay Bridge Tunnel.

Hs and Hmax of the AWAC the and buoy compare very favorably throughout the duration of the deployment. There are several spikes of Hmax that the buoy reports. These are suspect because the sample-to-sample consistency is fairly low (i.e. the peaks look like outliers). The AWAC was measuring waves at twice the frequency of the buoy (30 minutes compared to hourly) and thus resolves smaller features of the evolving wave field. Hmax was typically 0.3 to 0.4 m larger than Hs.

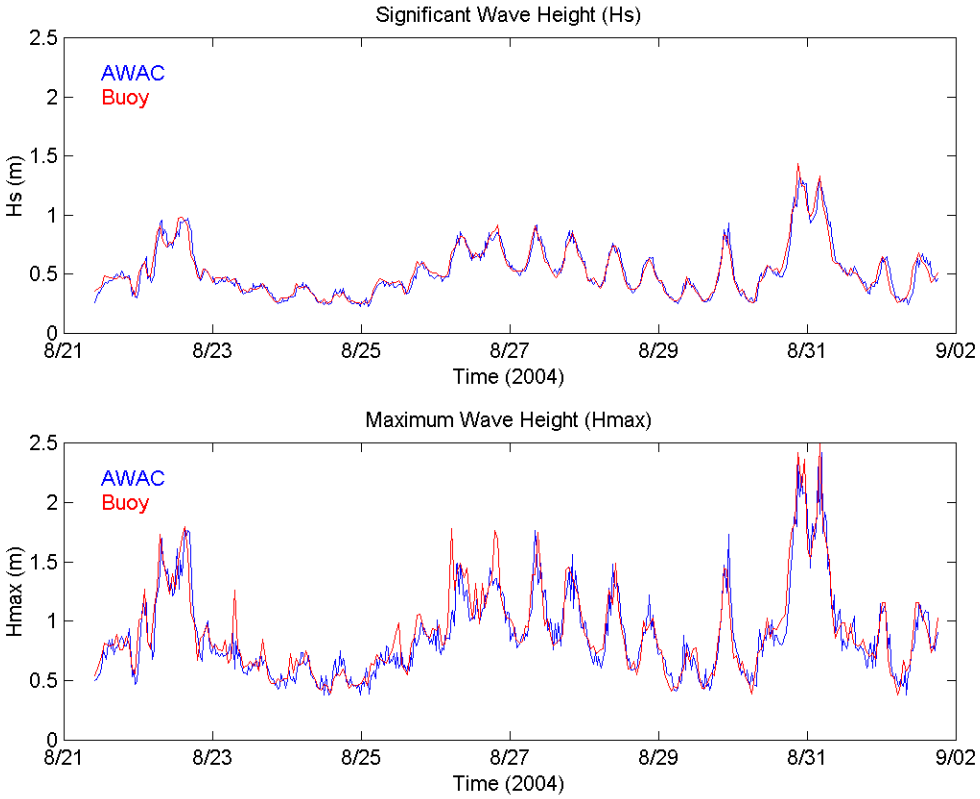

Figure 3. Significant wave height (Hs) and maximum wave height (Hmax) calculated for the AWAC and wave buoy.

Figure 4 gives the mean period (Tm), mean direction (DirTm), peak period (Tp) and peak direction (DirTp) for the AWAC and the buoy. While the overall pattern of the mean period is comparable between the AWAC and buoy, the average Tm of the AWAC was substantially lower than the buoy by typically 0.5 to 1.0 seconds. This difference is simply an artifact of frequency limitations inherent in each sampling method.

The wave buoy has a natural resonance frequency of about 1 second leading to a resolvable frequency range that is truncated to 0.64 Hz (about 1.6 seconds). The inherent frequency limitation of the AWAC is controlled by the footprint of the

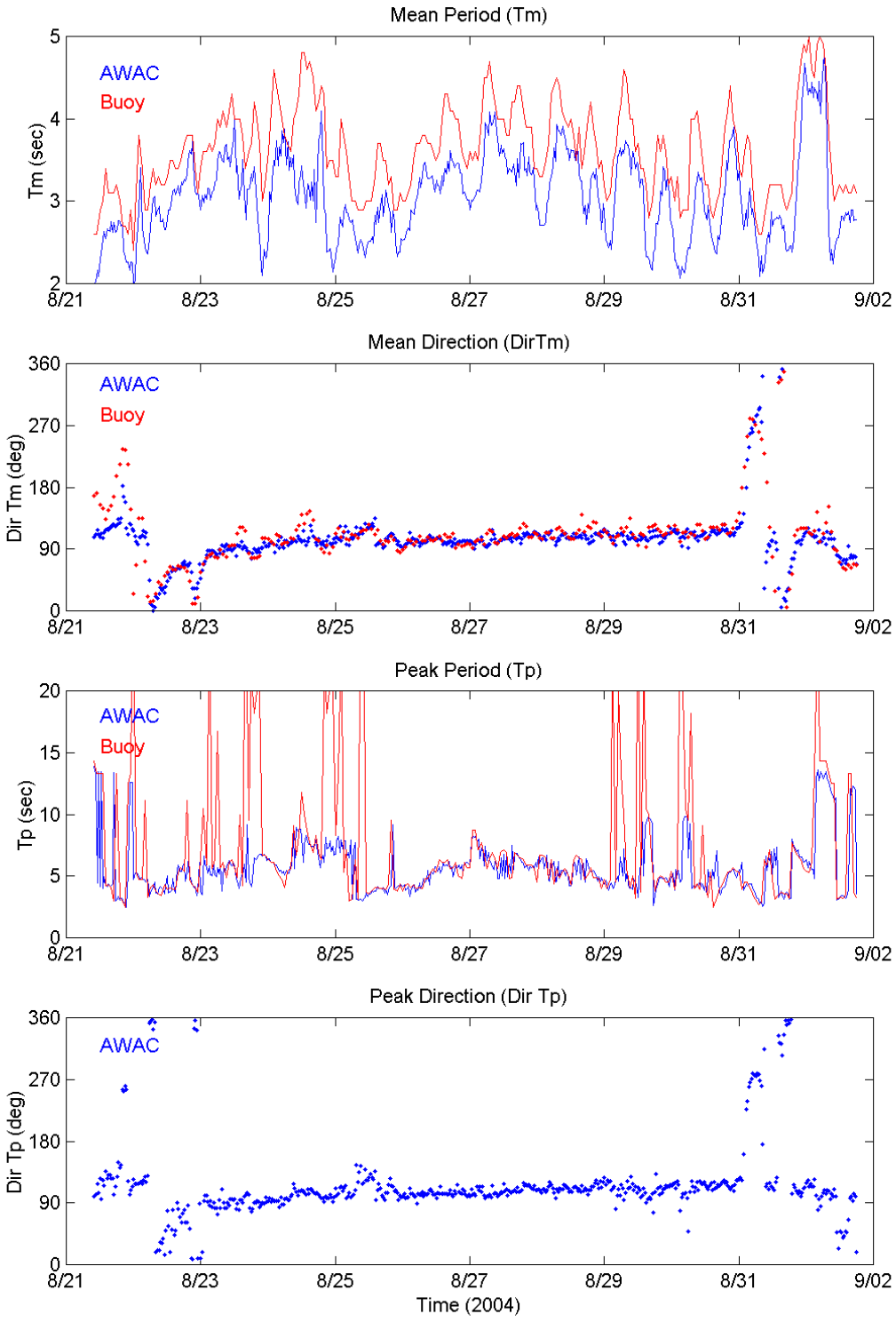

Figure 4. AWAC and buoy mean period (Tm), mean direction (DirTm), peak period (Tp) and peak direction (DirTp, AWAC only).

vertical beam as a function of range or deployment depth. For instance, at an average depth of 20 m (as in the case of this deployment), the AWAC vertical acoustic beam has a footprint of about 0.6 m. Using linear wave theory, this gives a Nyquist frequency limitation of 1.1 Hz (about 0.9 seconds). As such, the AWAC is capable of resolving waves of shorter period than the buoy, resulting in a lower mean period.

The mean direction of the AWAC and buoy compare quite closely. The typical wave direction is about 100 degrees which is consistent with waves entering the Chesapeake Bay from the Atlantic Ocean. The wave direction changed at the beginning and end of the record when larger frontal systems passed nearby, thus making the locally generated wind waves become the peak signal, and rotating direction as the fronts moved though the area.

The peak period during the deployment ranged from about 3 seconds to almost 15 seconds, with a typical value of about 5 seconds. While the overall pattern of peak period compared well between the AWAC and the buoy, the buoy logged several very large (over 20 seconds) peak periods. Waves with peak periods of this magnitude are not common in the rather protected waters of the Chesapeake Bay during the summer. These large peak periods have poor sample to sample consistency and are thought to be either electrical problems with the buoy or incorrect statistical calculations.

The wave buoy does not calculate peak direction, so the AWAC DirTp is plotted alone. Peak direction and mean direction were quite similar during this deployment and in the study region.

Figure 5 offers the scatter plot relation between the AWAC and buoy for Hs, Hmax, Tm, Tp and DirTm. The Hs and Hmax show no substantial difference between the AWAC and buoy over the range of values. The thin dashed lines on the Hs scatter plot indicate wave height differences of ± 5 cm. In total, 76% of the AWAC and Buoy Hs estimates were within ± 5 cm of each other (96% were within ± 10 cm).

The shift towards higher mean periods measured by the buoy is very evident in the scatter plot. It is also possible in this plot to see that the buoy only resolves mean period to 1/10 of a second (0.1 sec), while the AWAC has much higher temporal resolution of mean period. The bulk of the peak period values agree quite well, but the (likely) erroneous large peak period values observed by the buoy are apparent. Finally, mean direction is quite similar.

The AWAC frequency diagram (Fig. 6) shows the distribution of energy for small and large waves in the same time history. Each of the plotted spectra (each wave burst) are normalized between 0 and 1. The sense of amplitude can be understood from the overlying plot of Hs.

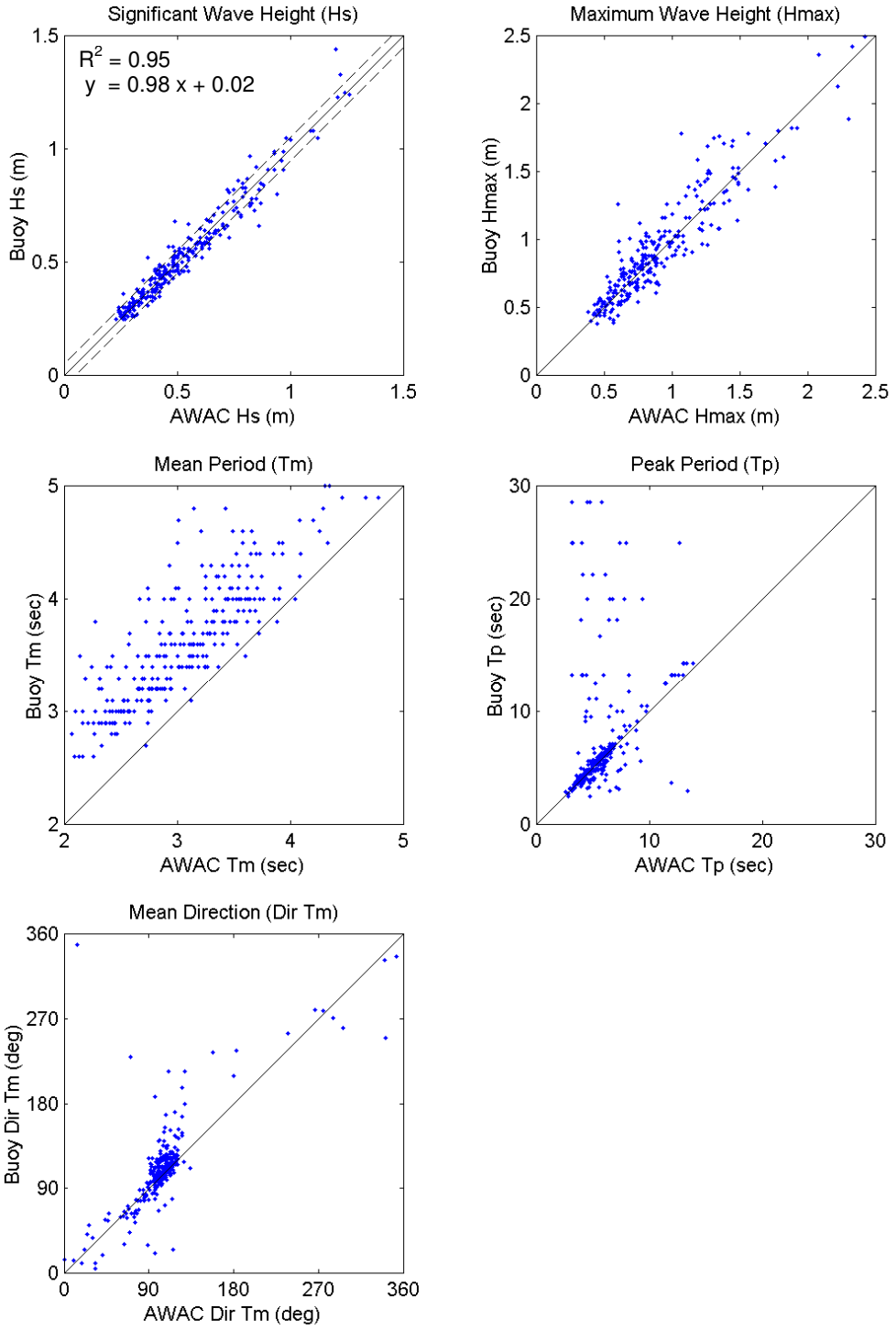

Figure 5. Scatter plots comparing AWAC and buoy Hs, Hmax, Tm, Tp and DirTm. Thin dashed lines on the Hs plot indicate ± 5 cm wave height.

Most of the wave energy was concentrated between 3 and 10 seconds. At the beginning and end of the record, very low frequency waves (more than 10 second period) were observed. These low frequency waves were likely generated from remote storms. The more typical 3-10 second waves were likely generated from local wind events.

The frequency diagram is a nice way to view complex wave structure over long time scales. Details that are more recognizable include persisting or waning wind events, the presence of ocean swell and the evolution of wave events from passing frontal systems. While very short waves (less than 2 second period) were not common during this deployment, there was a fair bit of energy in the 2-3 second period range.

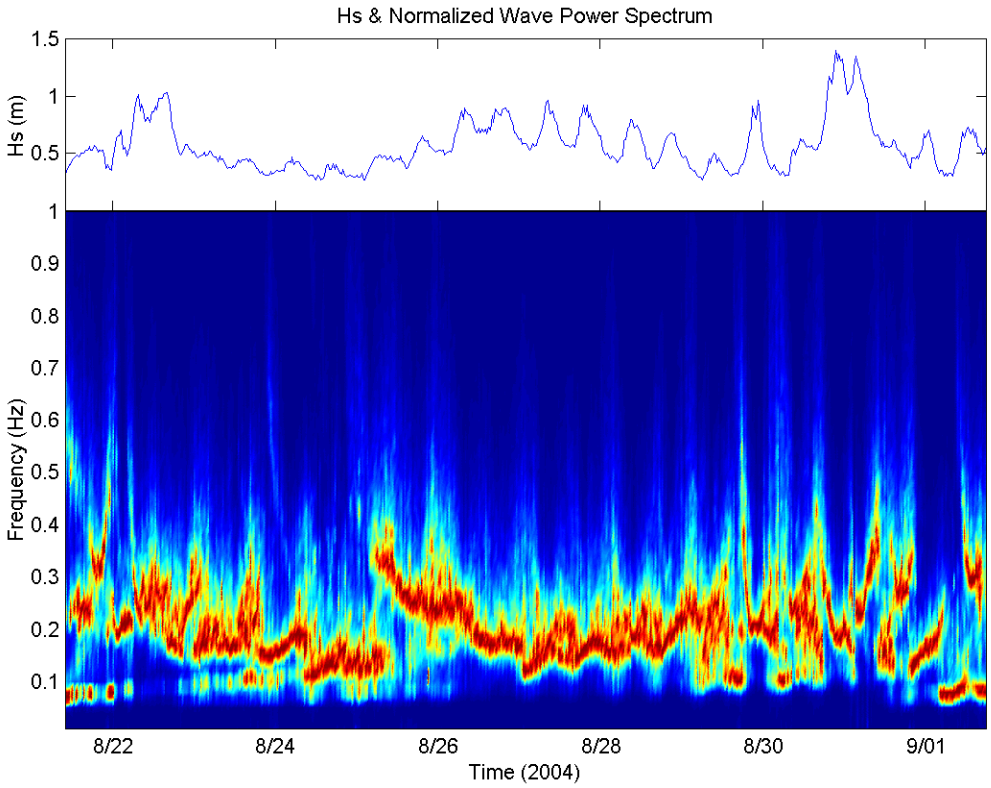

Figure 6. AWAC normalized wave frequency diagram and significant wave height (Hs).

Figure 7 gives two examples of the AWAC's acoustic surface tracking (AST) capabilities. The top pane is a 125 second portion of wave burst number 457 (500 samples at 4 Hz, ~2 minutes). This was on 30 August at 2200 hours, a time of large wave heights (order 2 m). The blue line gives the AST time series measured at 4 Hz. The red line gives the pressure record measured at 2 Hz.

The bottom pane shows a portion of the AST and pressure time series during wave burst number 178 (25 August at 0300 hours); a period of small waves (order 0.2 m). In both panes, it is evident that the pressure signal is greatly attenuated at depth (about 20 m). As a result, the pressure signal does not resolve as much of the fine detail of wave height and form as does the AST. This deployment shows the effectiveness of the AST in measuring wave height time series from 20 m depth for both large wave (with breaking tops and bubbles) and small, short wave conditions.

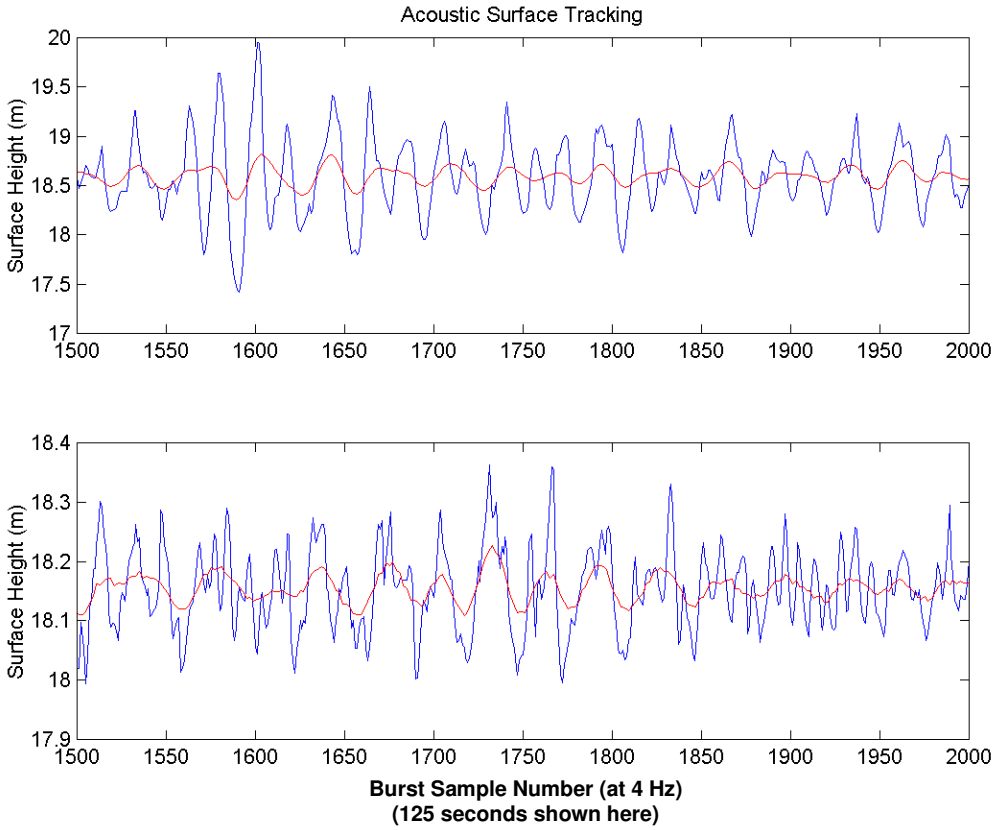

Figure 7. Time series of AWAC acoustic surface tracking (AST, blue) and pressure (red) during wave burst 457 (top) and 178 (bottom). Note different y-scales.

Figure 8 gives the energy density spectra of wave height from the two burst samples shown in Figure 8 for the AWAC and the buoy. The top plot suggests that the AWAC and the wave buoy calculated similar spectra during the large wave event. The AWAC measured a peak period of 5.53 seconds and a significant wave height of 1.33 m.

The lower plot of Figure 8 reports the wave height spectra during small wave conditions. The AWAC reports Tp of 7.17 seconds and Hs of 0.24 m. During the

small wave conditions, the AWAC resolves energy fairly equally distributed around the peak period. The wave buoy does not display a single prominent range of high energy. Rather, it shows several distinct peaks scattered across the frequency range. Further analysis is required to determine whether this is a true observation or simply indicates the noise level of the wave buoy during small wave conditions.

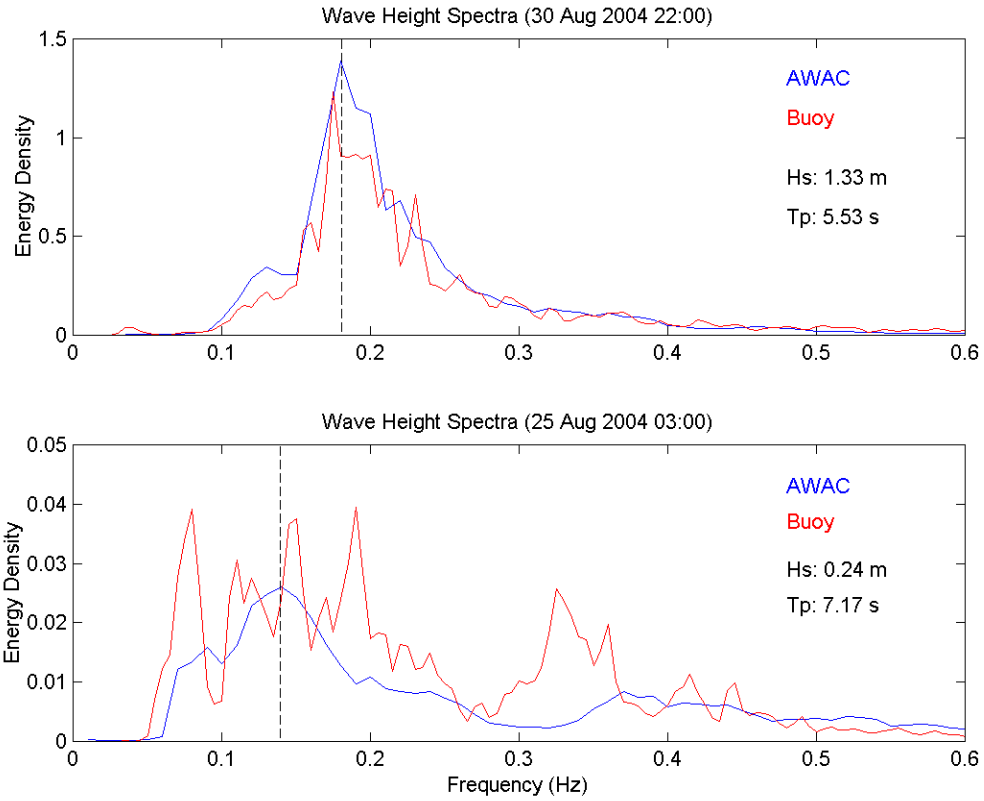

Figure 8. Energy density spectra of wave height for AWAC (blue) and Buoy (red) at same times as given in Figure 8. AWAC Hs and Tp (dashed line) are given for reference. Note different y-scales.

Figure 9 gives the contour plots of the U and V components of velocity as measured by the AWAC. The semi-diurnal tidal cycle (bold black line) is clearly evident in both the U and V components of velocity. Larger tidal velocities were measured in the U component which is consistent with the ebbing and flooding of the Chesapeake Bay. Typical tidal velocities reach a maximum speed of about 1 m/s.

The large wind/wave events at the beginning (8/22) and end (8/31) of the deployment are clearly visible in the current record as high U and V velocities. During these events, current speeds reached 1.5 m/s. The usual tidal current pattern was largely modified by the external forcing. For example, the U

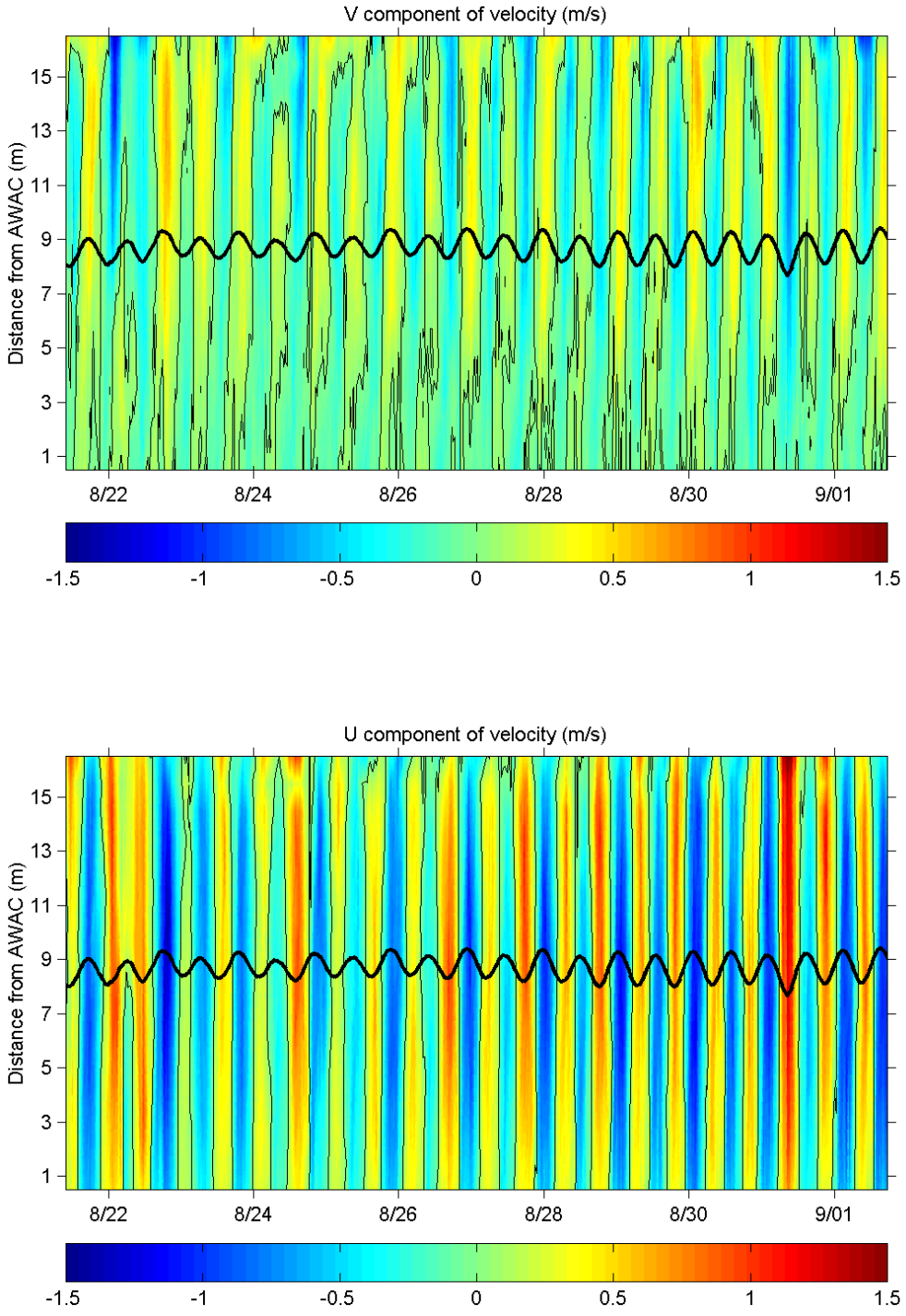

Figure 9. Contour plots of V component (North/South) and U component (East/West) of velocity measured by the AWAC (m/s). Thin black lines indicate the zero velocity contour. Bold black line indicates sea level (minus 10 m to fit on y-scale).

component of the flood tide on 8/22 (negative velocity, blue color) is dampened near the surface and the flow is actually reversed (positive flow, yellow color).

To gain insight into how much energy each frequency band contributes to the total energy, the kinetic energy distribution fraction (EDF) is presented in Figure 10 for near-surface and near-bottom currents. These plots are integrated and normalized spectral density functions showing the partition of the kinetic energy over the different frequency bands.

The EDF corroborates that, as observed in the velocity contour plots, most of the energy in the U component of velocity is constrained to the semi-diurnal band (M_2 tidal constituent, 12.42 hours). This is particularly true for near-bottom U velocities as they may be less affected by surface wind forcing. Nearly 85% of the total energy in the near-bottom U component of velocity is constrained to the semi-diurnal band (the semi-diurnal band accounts for about 50% of all energy near-surface).

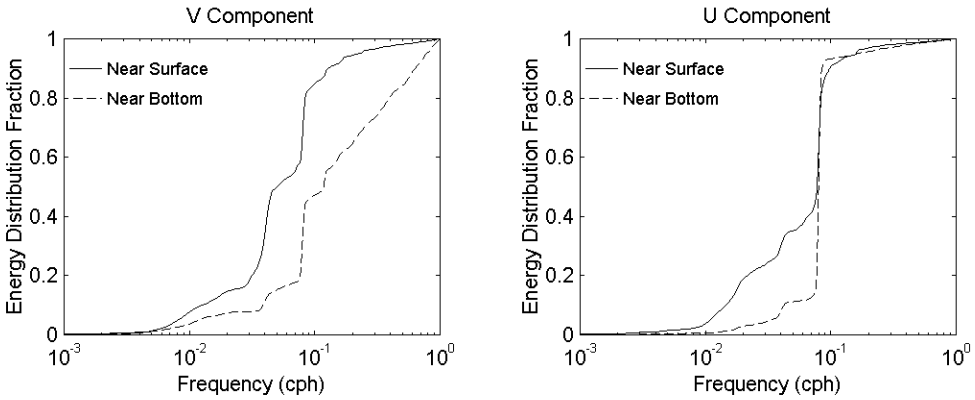

Figure 10. Energy Distribution Fraction (EDF) of V and U components of velocity at cell 1 (near bottom) and cell 17 (near surface).

The near-bottom V component of velocity shows quite a bit of high frequency energy. About 25% of the energy is centered on the semi-diurnal band. The near-surface plot shows about equal distribution of power around the semi-diurnal and diurnal bands (~25% each).

Both of the near-surface U and V components of velocity have more energy in the lower frequency (synoptic) bands than the near-bottom currents. This is consistent with low frequency wind forcing preferentially near the top of the water column. On average, about 20% of all energy is located in these low frequency synoptic bands.

Figure 11 shows the profiles of mean current speed and direction over the deployment period. As expected in a tidally dominated area, the mean current speed is very low and not substantially different from zero. However, the structure of the mean current speed and direction agrees with general estuarine circulation theory. The estuarine exchange flow is evident in the mean current direction plot. Near-surface currents are directed out-estuary (East of South) and near-bottom currents are directed in-estuary (West of South).

Boundary and mixed layers could be inferred though these mean speed and direction plots. A bottom boundary layer on the order of 5 m is observed. The surface mixed layer is roughly 8 m deep. While these are reasonable estimates for estuary environments, salinity and density profiles would be required to confirm layer structure.

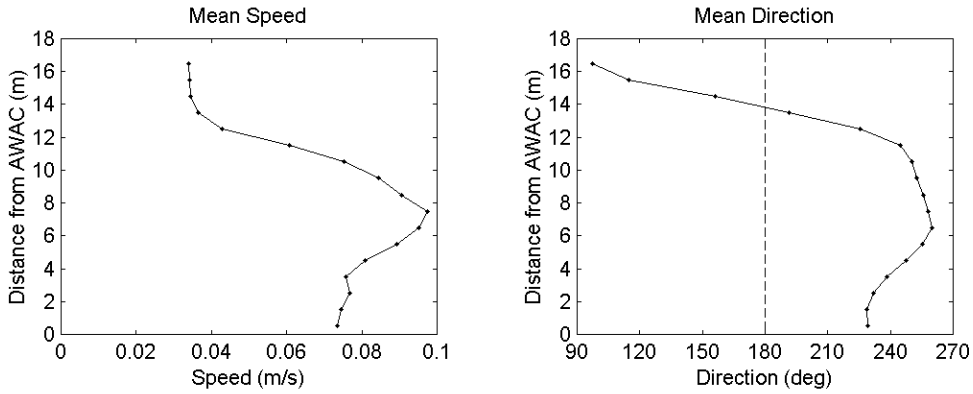

Figure 11. Profile of mean current speed and direction as measured by the AWAC. The vertical dashed line denotes Southward flow.